

## Analysis of a Shil'nikov Type Homoclinic Bifurcation

**Yan Cong XU**

*Department of Mathematics, Hangzhou Normal University, Hangzhou 310036, P. R. China*  
*E-mail: yancongx@163.com*

**Xing Bo LIU<sup>1)</sup>**

*Department of Mathematics, Shanghai Key Laboratory of PMMP, East China Normal University,  
Shanghai 200241, P. R. China*  
*E-mail: xbliu@math.ecnu.edu.cn*

**Abstract** The bifurcation associated with a homoclinic orbit to saddle-focus including a pair of pure imaginary eigenvalues is investigated by using related homoclinic bifurcation theory. It is proved that, in a neighborhood of the homoclinic bifurcation value, there are countably infinite saddle-node bifurcation values, period-doubling bifurcation values and double-pulse homoclinic bifurcation values. Also, accompanied by the Hopf bifurcation, the existence of certain homoclinic connections to the periodic orbit is proved.

**Keywords** Homoclinic bifurcation, Hopf bifurcation, Poincaré map

**MR(2010) Subject Classification** 34C23, 34C37, 37C29

### 1 Introduction and Hypotheses

In the past few decades, the research on bifurcations of various dynamical systems has made great progress. Bifurcation theory has attracted lots of attention due to its important role in applications to many subjects (see [1–24], and the references therein). An overview of homoclinic and heteroclinic bifurcation theory for autonomous vector fields is given in Homburg and Sandstede [12]. It is known from the pioneering works of [17, 18] that homoclinic connections are important organizing centers of the three dimensional autonomous dynamical systems and that can lead to a very rich dynamical behaviors.

One of them is the orbit homoclinic to a fixed point of saddle-focus type of the three dimensional system. This is known as the Shil'nikov phenomena since it was first studied by Shil'nikov [17].

Belykov [3] analyzed a three dimensional system whose principal homoclinic connection is inside the Shil'nikov region, where the saddle index  $\delta = -\frac{\lambda}{\gamma} < 1$ . Belykov [4] studied the codimension-two problem of a homoclinic orbit to a saddle-focus equilibrium that is close to the border of the Shil'nikov region, that is,  $\delta = 1$ . Algaba et al. [1, 2] considered the homoclinic connection for system with  $Z_2$ -symmetry inside the Shil'nikov region.

---

Received April 9, 2015, accepted September 6, 2017

Supported by National NSF (Grant Nos. 11371140, 11671114) and Shanghai Key Laboratory of PMMP

1) Corresponding author

The symbolic dynamics of  $\delta = 0$  were firstly analyzed by Hirschberg and Knobloch [11], they derived a 2-parameter Poincaré map modeling a 3-dimensional vector flow near the codimension-2 point defined by a Shil’nikov homoclinic orbit to a fixed point undergoing a Hopf bifurcation. The map is analyzed finding primary homoclinic tangencies to the small Hopf cycle. Parameter dependence of periodic orbits associated with these tangencies is described. Global behavior of the tube-like unstable manifold of the Hopf cycle is studied in depth, analytically and numerically, locating its simplest subsidiary tangencies. Deng and Sakamoto [7] also carried out a detailed geometric analysis to a general codimension-two Shil’nikov–Hopf bifurcation by setting up local, global poincaré maps and using Lyapunov–Schmidt reduction. Champneys et al. [5] added a non-transverse parametric condition to system (1.1), investigated the codimension-three Shil’nikov–Hopf bifurcation caused by the non-transverse, i.e., degenerately parametrically unfolded, Shil’nikov–Hopf bifurcation, and it contained nearby dynamics akin to both degeneracies.

In this work, by using the technique of bifurcation theory, we will focus on the global analysis on the following three dimensional autonomous system:

$$\begin{cases} \dot{x} = \lambda x - \omega y + P(x, y, z, \mu), \\ \dot{y} = \omega x + \lambda y + Q(x, y, z, \mu), \\ \dot{z} = \gamma z + R(x, y, z, \mu), \end{cases} \tag{1.1}$$

where  $P, Q, R$  are  $C^r (r \geq 2)$  and  $O(2)$  at the origin  $O(0, 0, 0)$ .  $O(0, 0, 0)$  is a saddle-focus type stationary point; i.e., the eigenvalues of system (1.1) linearied about  $(0, 0, 0)$  are given by  $\lambda \pm i\omega, \gamma$  with  $\lambda \leq 0 < \gamma$  and  $\omega > 0$ .

Our main aim in this paper is to provide a geometric analysis that unfolds the dynamics near the homoclinic cycle connecting nonhyperbolic equilibrium with a pair of pure imaginary eigenvalues. It is proved that, in a neighborhood of the homoclinic bifurcation value, there are countably infinite saddle-node bifurcation values, period-doubling bifurcation values and double-pulse homoclinic bifurcation values. Also, accompanied by the Hopf bifurcation, the existence of certain homoclinic connections to the periodic orbit is proved.

A common tool in analyzing these problems is to define a suitable codimension 1 transversal section to the homoclinic cycle and further define two mappings whose composition gives a Poincaré map. With the construction of this return map it is possible to derive information on periodic orbit bifurcations as well as homoclinic bifurcations (see Shilnikov [17], Glendinning and Sparrow [9]). The technique of analysis in this paper is also given in Wiggins [20].

Next we consider system (1.1) with the following hypotheses.

(H<sub>1</sub>) Near  $O(0, 0, 0)$  it is possible to choose coordinates  $(x, y, z)$  in such a way that the flow, in a neighborhood of this equilibrium, is generally defined by the equations

$$\begin{cases} \dot{r} = r(\lambda - r^{2k}), \\ \dot{\theta} = \omega, \\ \dot{z} = \gamma z, \end{cases}$$

where  $(r, \theta)$  are the polar coordinates of  $(x, y)$ , and  $\lambda$  is the principal parameter of the Hopf bifurcation.

Let  $C$  be the periodic orbit that emerges, for  $\lambda > 0$ , from the Hopf bifurcation of  $O(0, 0, 0)$ .

(H<sub>2</sub>) When  $\lambda = \mu = 0$ , system (1.1) possesses a homoclinic orbit  $\Gamma$  connecting  $O(0, 0, 0)$  to itself.

The paper is organized as follows. In Section 2, we establish the bifurcation equations by constructing the local and global Poincaré maps. In Section 3, by the analysis of the bifurcation equations, we know that, in a neighborhood of the homoclinic bifurcation value, there are countably infinite saddle-node bifurcation values, period-doubling bifurcation values and double-pulse homoclinic bifurcation values. Also, accompanied by the Hopf bifurcation, the existence of certain homoclinic connections to a periodic orbit is proved.

### 2 The Construction of the Poincaré Map

By [17, 24], we know that near the equilibrium  $O(0, 0, 0)$ , system (1.1) can be written in the following form (in polar coordinates with  $x = r \cos \theta$ ,  $y = r \sin \theta$ )

$$\begin{cases} \dot{r} = r(\lambda - r^{2k}) + P_k(r, \theta, z, \mu), \\ \dot{\theta} = \omega + b_1 r^2 + \dots + b_k r^{2k} + Q_k(r, \theta, z, \mu), \\ \dot{z} = \gamma z + z(g_1 r^2 + \dots + g_k r^{2k}) + H_k(r, \theta, z, \mu), \end{cases} \tag{2.1}$$

where  $P_k, H_k = O(2k + 2)$ ,  $Q_k = O(2k + 1)$ ,  $P_k(0, \theta, z, \mu) = H_k(r, \theta, 0, \mu) = 0$  in the neighborhood of  $O$ .  $O(n)$  represents the order is  $n$  at origin with respect to  $r, z$ .

Set up the following two Poincaré sections  $\Sigma_0$  and  $\Sigma_1$ :

$$\begin{aligned} \Sigma_0 &= \{(x, y, z) | y = 0, \varepsilon_1 < x \leq \varepsilon, 0 \leq z < \varepsilon\}, \\ \Sigma_1 &= \{(x, y, z) | z = \varepsilon\}, \end{aligned}$$

where  $\varepsilon$  and  $\varepsilon_1$  are small enough positive numbers (see Figure 1).

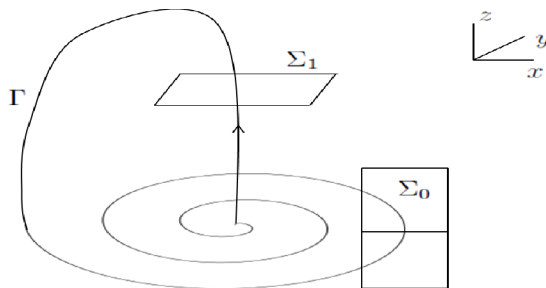


Figure 1 The saddle-focus homoclinic cycle and construction of cross sections

An approximately local Poincaré map from  $\Sigma_0$  to  $\Sigma_1$  is constructed by assuming that the dynamics inside the box  $\{x \leq \varepsilon, y \leq \varepsilon, 0 \leq z \leq \varepsilon\}$  are governed by the truncated equations

$$\begin{cases} \dot{r} = r(\lambda - r^{2k}), \\ \dot{\theta} = \omega, \\ \dot{z} = \gamma z. \end{cases}$$

By integrating the flow close to the equilibrium, we obtain the following local Poincaré map

$$T_0 : \Sigma_0 \rightarrow \Sigma_1, \quad (x_0, 0, z_0) \rightarrow (x_1, y_1, \varepsilon),$$

where

$$\begin{aligned}
 x_1 &= R(x_0, \tau(z_0), \lambda) \cos \left[ \frac{\omega}{\gamma} \ln \frac{\varepsilon}{z_0} \right], \\
 y_1 &= R(x_0, \tau(z_0), \lambda) \sin \left[ \frac{\omega}{\gamma} \ln \frac{\varepsilon}{z_0} \right], \\
 \tau(z_0) &= \frac{1}{\gamma} \ln \frac{\varepsilon}{z_0}, \\
 R(x_0, \tau(z_0), \lambda) &= \begin{cases} x_0 e^{\lambda \tau} \left[ 1 + 2k\tau x_0^{2k} \frac{\sinh(k\tau)}{k\lambda\tau} e^{k\lambda\tau} \right]^{-\frac{1}{2k}}, & \lambda \neq 0, \\ x_0 (1 + 2k\tau x_0^{2k})^{-\frac{1}{2k}}, & \lambda = 0, \end{cases}
 \end{aligned} \tag{2.2}$$

and  $\tau(z_0)$  is the time of flight from  $\Sigma_0$  to  $\Sigma_1$ .

We now consider  $\Sigma_0$  more carefully. For  $\Sigma_0$  arbitrarily chosen it is possible for points on  $\Sigma_0$  to intersect  $\Sigma_0$  many times before reaching  $\Sigma_1$ . Note that, it takes time  $t = \frac{2\pi}{\omega}$  for a point starting in the  $x - z$  plane with  $x > 0$  to return to the  $x - z$  plane with  $x > 0$ . Now let  $x = \varepsilon, 0 \leq z \leq \varepsilon$  be the right-hand boundary of  $\Sigma_0$ . Then if we choose  $x = \varepsilon(1 + \frac{4k\pi\varepsilon^{2k}}{\omega})^{-\frac{1}{2k}}, 0 \leq z \leq \varepsilon$  to be the left-hand boundary of  $\Sigma_0$ , no point starting in the interior of  $\Sigma_0$  returns to  $\Sigma_0$  before reaching  $\Sigma_1$ . It is possible for points on  $\Sigma_0$  to intersect  $\Sigma_0$  many times before reaching the section  $\Sigma_1$ . To avoid this situation, we should assume some other restrictions for  $\Sigma_0$ , thus we take  $\varepsilon_1$  satisfying

$$\varepsilon \left( 1 + \frac{4k\pi\varepsilon^{2k}}{\omega} \right)^{-\frac{1}{2k}} < \varepsilon_1 < \bar{x} \leq \varepsilon,$$

where  $(\bar{x}, 0, 0)$  is one of the infinitely many intersections of the homoclinic cycle  $\Gamma$  with  $\Sigma_0$ .

We now consider the map  $T_1 : \Sigma_1 \rightarrow \Sigma_0$ . The time of flight is finite for the map  $T_1$  since we are outside of a neighborhood of the stationary point  $O(0, 0, 0)$ . The map  $T_1$  can be obtained by neglecting the higher-order terms in the Taylor expansion of the flow between  $\Sigma_1$  and  $\Sigma_0$ . Of course, this approximation to  $T_1$  introduces an error. However, in Wiggins [20] it is shown that, by continuity with respect to initial conditions, for  $\Sigma_1$  sufficiently small, the flow generated by the vector field maps  $\Sigma_1$  onto  $\Sigma_0$ . This implies that the higher-order terms in Taylor expansion can be made arbitrarily small. So the error is truly negligible in the sense that it does not affect our results. Then similar to that in Wiggins [20], the map  $T_1$  can be written as

$$\begin{aligned}
 T_1 : \Sigma_1 &\rightarrow \Sigma_0, \quad (x_1, y_1, \varepsilon) \rightarrow (x, 0, z), \\
 \begin{pmatrix} x_1 \\ y_1 \\ \varepsilon \end{pmatrix} &\rightarrow \begin{pmatrix} \bar{x}(\mu) \\ 0 \\ \bar{z}(\mu) \end{pmatrix} + \begin{pmatrix} a & b & 0 \\ 0 & 0 & 0 \\ c & d & 0 \end{pmatrix} \begin{pmatrix} x_1 \\ y_1 \\ 0 \end{pmatrix} = \begin{pmatrix} x \\ 0 \\ z \end{pmatrix},
 \end{aligned}$$

where  $(\bar{x}(0) = \bar{x}, \bar{z}(0) = 0, a, b, c, d$  are constants and  $ad - bc \neq 0$ . Let us briefly explain the form of  $T_1$ . Since  $\bar{x} \neq 0$ , then the term with respect to small parameter  $\mu$  can be neglected in the first row. On  $\Sigma_0$  the  $y$  coordinate is fixed at  $y = 0$ . This explains why there are only zeros in the middle row of the linear part of  $T_1$ . Also, the  $z$  coordinate of  $\Sigma_1$  is fixed at  $z = \varepsilon$ . This explains why there are only zeros in the third column of the matrix in  $T_1$ .

Further we assume

$$(H_3) \quad \bar{z}'(0) \neq 0.$$

Now the map  $T_1$  can be simplified into the following form

$$\begin{aligned} x &= \bar{x} + ax_1 + by_1, \\ z &= \mu + cx_1 + dy_1. \end{aligned} \tag{2.3}$$

Then the first return map

$$T = T_1 \circ T_0 : \Sigma_0 \rightarrow \Sigma_0$$

is now obtained from the expressions of  $T_1$  and  $T_0$ , that is,

$$\begin{aligned} x &= \bar{x} + R(a \cos \theta_0 + b \sin \theta_0), \\ z &= \mu + R(c \cos \theta_0 + d \sin \theta_0), \end{aligned} \tag{2.4}$$

where  $\theta_0 = \frac{\omega}{\gamma} \ln \frac{\varepsilon}{z_0}$ . For convenience, we give some new notations.

Define

$$\begin{aligned} \Omega &= -\frac{\omega}{\gamma}, \quad A_1 = \sqrt{a^2 + b^2}, B_1 = \sqrt{c^2 + d^2}, \quad \delta = -\frac{\lambda}{\gamma}, \quad v_0 = \frac{z_0}{\varepsilon}, \\ a \cos \theta_0 + b \sin \theta_0 &= A_1 \cos(\theta_0 + \phi_1), \quad c \cos \theta_0 + d \sin \theta_0 = B_1 \sin(\theta_0 + \phi_2), \\ \theta_1 &= \phi_1 - \Omega \ln \varepsilon, \quad \theta_2 = \phi_2 - \Omega \ln \varepsilon. \end{aligned}$$

Then combining with (2.4), we obtain

$$T : \Sigma_0 \rightarrow \Sigma_0, \quad \begin{pmatrix} x \\ z \end{pmatrix} = \begin{pmatrix} \bar{x} + RA_1 \cos(\Omega \ln z_0 + \theta_1) \\ \mu + RB_1 \sin(\Omega \ln z_0 + \theta_2) \end{pmatrix}. \tag{2.5}$$

After some rescaling  $z \rightarrow ze^{-\frac{\Omega}{\omega}\theta_2}$ , we finally obtain the following expression for the Poincaré map

$$T : \Sigma_0 \rightarrow \Sigma_0, \quad \begin{pmatrix} x \\ z \end{pmatrix} = \begin{pmatrix} \bar{x} + FA_1 \cos(\Omega \ln z_0 + \theta) \\ \mu + FB_1 \sin(\Omega \ln z_0) \end{pmatrix}, \tag{2.6}$$

where  $\theta = \theta_1 - \theta_2$ ,  $v_0 = \frac{z_0}{\varepsilon} e^{-\frac{\Omega}{\omega}\theta_2}$ , and

$$F(x_0, z_0, \lambda) = \begin{cases} x_0 v_0^{-\delta} \left[ 1 + \frac{x_0^{2k}}{\lambda} (v_0^{-2k\delta} - 1) \right]^{-\frac{1}{2k}}, & \lambda \neq 0, \\ x_0 \left( 1 - 2k \frac{x_0^{2k}}{\gamma} \ln v_0 \right)^{-\frac{1}{2k}}, & \lambda = 0. \end{cases}$$

Also, the function  $F(x_0, z_0, \lambda)$  satisfies the following properties

$$\begin{aligned} \lim_{z_0 \rightarrow 0} F(x_0, z_0, \lambda) &= 0, \quad \lambda \leq 0, \\ \lim_{z_0 \rightarrow 0} F(x_0, z_0, \lambda) &= \sqrt[2k]{\lambda}, \quad \lambda > 0. \end{aligned}$$

### 3 The Bifurcation Results

Firstly, we consider the case  $\lambda = 0$ , we will study the fixed points of the Poincaré map (2.6), and give a global analysis about the different phenomena. Now  $(x, z)$  is the fixed point of the Poincaré map (2.6) if and only if

$$\begin{aligned} x &= \bar{x} + F(x, z)A_1 \cos(\Omega \ln z + \theta), \\ z &= \mu + F(x, z)B_1 \sin(\Omega \ln z). \end{aligned} \tag{3.1}$$

Solving the first equation for  $x$  as a function of  $z$  and substituting it into the second equation, then combining with  $F(x, z) \rightarrow (-\frac{2k}{\gamma} \ln v)^{-\frac{1}{2k}}$  as  $z \rightarrow 0$  small enough, where  $v = \frac{z}{\varepsilon} e^{-\frac{\gamma}{\omega} \theta_2}$ , the mentioned-above equations become

$$z = \mu + \left(-\frac{2k}{\gamma} \ln v\right)^{-\frac{1}{2k}} B_1 \sin(\Omega \ln z). \tag{3.2}$$

Solving (3.2) gives us the  $z$ -component of the fixed point, substituting this into (3.1) gives us the  $x$ -component of the fixed point. Denote

$$K(z) = z - \mu, \quad G(z) = \left(-\frac{2k}{\gamma} \ln v\right)^{-\frac{1}{2k}} B_1 \sin(\Omega \ln z).$$

Then system (1.1) has periodic orbit if and only if the line  $L_1 : \xi = K(z)$  and the wiggly curve  $L_2 : \xi = G(z)$  have intersection points as  $0 < z \ll 1$ .

By the amplitude function  $H(z) = B_1(-\frac{2k}{\gamma} \ln v)^{-\frac{1}{2k}}$ , we have  $\frac{\partial H}{\partial z} \rightarrow \infty$  as  $z \rightarrow 0$ , then the line  $L_1$  and the curve  $L_2$  have countable infinity many fixed points as  $\mu = 0$ , and have finite number of fixed points as  $0 < \mu \ll 1$ . Also, the corresponding periodic orbits have longer period as  $z \rightarrow 0$ .

Next, we consider the stability of the bifurcated periodic orbits. It is desirable to calculate some of the stability properties of the fixed points of (3.1) (and hence of the periodic orbits on which they lie). Our analysis is only partial, but tells us all we need to know. The Jacobian matrix of the map (3.1) is given by

$$DT = \begin{pmatrix} D_1 & D_2 \\ D_3 & D_4 \end{pmatrix},$$

where  $f = (\ln \frac{\varepsilon}{z})^{-\frac{1}{2k}}$ , and

$$\begin{aligned} D_1 &= O\left(1 + 2k \frac{x^{2k}}{\gamma} \ln \frac{\varepsilon}{z}\right)^{-\frac{1}{2k}} \cos(\Omega \ln z + \theta), \\ D_2 &= A_1 f \left(-\frac{2k}{\gamma}\right)^{-\frac{1}{2k}} z^{-1} \left[\frac{1}{2k} f^{2k} \cos(\Omega \ln z + \theta) - \Omega \sin(\Omega \ln z + \theta)\right], \\ D_3 &= O\left(1 + 2k \frac{x^{2k}}{\gamma} \ln \frac{\varepsilon}{z}\right)^{-\frac{1}{2k}} \sin(\Omega \ln z), \\ D_4 &= B_1 f \left(-\frac{2k}{\gamma}\right)^{-\frac{1}{2k}} z^{-1} \left[\frac{1}{2k} f^{2k} \sin(\Omega \ln z) + \Omega \cos(\Omega \ln z)\right]. \end{aligned}$$

Suppose  $(x_p, z_p)$  is a fixed point of the map  $T$ , then the eigenvalues of the corresponding Jacobian matrix are given by

$$\lambda_{1,2} = \frac{1}{2}[(D_1 + D_4) \pm \sqrt{(D_1 + D_4)^2 - 4(D_1 D_4 - D_2 D_3)}].$$

Thus a fixed point  $(x_p, z_p)$  corresponding to a zero crossing of this wiggly curve implies  $D_3 = 0$ . In this case,  $\lambda_1 = D_1$ ,  $\lambda_2 = D_4$ . So for  $0 < z \ll 1$ ,  $\lambda_1$  is small and  $\lambda_2$  is always large, thus the fixed point is a saddle.

Similarly, a fixed point corresponding to a maximum of this wiggly curve implies  $D_4 = 0$ . In this case

$$\lambda_{1,2} = \frac{1}{2}\left(D_1 \pm \sqrt{D_1^2 + 4D_2 D_3}\right).$$

By a simple computation, we know that  $|\lambda_{1,2}| \gg 1$ , thus the fixed point has two-dimensional unstable manifold.

Now we describe the following five cases at each parameter value (see Figure 2). The proof follows along the lines of the proof of Glendinning and Sparrow [9] (see also Wiggins [20] for details).

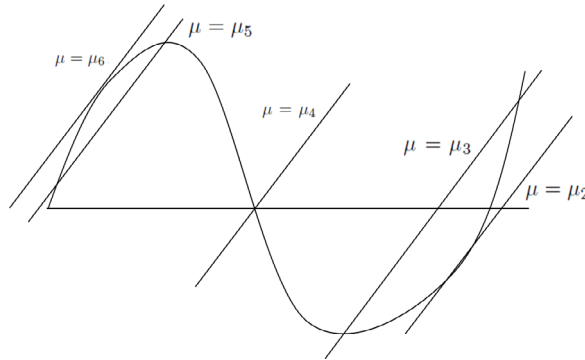


Figure 2 Illustration of different parameter values

(i)  $\mu = \mu_6$ . At this point we have a tangency, and we know that a saddle-node pair will be born in a saddle-node bifurcation.

(ii)  $\mu = \mu_5$ . At this point we have two fixed points; the one with the lower  $z$  value has the larger period. Also, the one at the maximum of the curve has  $D_4 = 0$ ; therefore, it is unstable node. The other fixed point is a saddle.

(iii)  $\mu = \mu_4$ . At this point, the fixed point is a saddle since  $D_3 = 0$ . Then there exists a parameter  $\mu = \mu^*$  between  $\mu_5$  and  $\mu_4$ , at  $\mu = \mu^*$ , it must have changed the stability type of fixed point via a period doubling bifurcation.

In fact, as the parameter  $\mu$  changes from  $\mu_5$  to  $\mu_4$ , the stability type of the fixed point is changed, then there must exist a bifurcation parameter  $\mu^*$  between  $\mu_5$  and  $\mu_4$ . But note that the numbers of the fixed point of the map  $T$  don't change, that is, the saddle-node bifurcation, transcritical bifurcation and pitchfork bifurcation can not happen, then the eigenvalues of  $DT$  do not equal to 1. If the eigenvalues  $\lambda_{1,2} = \frac{1}{2}(\text{tr}DT \pm \sqrt{(\text{tr}DT)^2 - 4\det(DT)})$  are a pair of complex conjugate eigenvalues, then by  $0 < z_p \ll 1$ , we have  $|\lambda_{1,2}| = \sqrt{\det DT} \gg 1$ . That means  $DT$  has no complex conjugate eigenvalues having modulus 1. Thus we can conclude one eigenvalue of  $DT$  equals to  $-1$ , which means a period-doubling bifurcation occurs.

(iv)  $\mu = \mu_3$ . At this point, the fixed point is at the minimum of the curve, then  $D_4 = 0$  again, therefore the saddle is changed into an unstable node. This must have occurred via a period-doubling bifurcation.

(v)  $\mu = \mu_2$ . At this point, a saddle-node bifurcation occurs.

Now we denote the parameter values of saddle-node bifurcations by

$$\mu_i, \mu_{i+1}, \dots, \mu_n, \dots \rightarrow 0,$$

where  $\mu_i \mu_{i+1} < 0$ .

Recall that the  $z$  component of the fixed point was given by the solutions to the equations

$$z - \mu = G(z) = H(z) \sin(\Omega \ln z),$$

so we have

$$\begin{aligned} z_i - \mu_i &= H(z_i) \sin(\Omega \ln z_i), \\ z_{i+1} - \mu_{i+1} &= H(z_{i+1}) \sin(\Omega \ln z_{i+1}). \end{aligned}$$

Since

$$\Omega \ln z_{i+1} - \Omega \ln z_i \approx \pi,$$

then it follows

$$\frac{z_{i+1}}{z_i} \approx \exp(\Omega^{-1} \pi),$$

it is easy to obtain

$$\begin{aligned} \frac{\mu_{i+1}}{\mu_i} &= \frac{z_{i+1} - H(z_{i+1}) \sin(\Omega \ln z_{i+1})}{z_i - H(z_i) \sin(\Omega \ln z_i)} \\ &\approx - \left[ \frac{\ln(\frac{\varepsilon}{z_i})}{\ln(\frac{\varepsilon}{z_{i+1}})} \right]^{\frac{1}{2k}} \approx -1. \end{aligned}$$

This quantity governs the size of the oscillations. That is, as  $\lambda = 0$ , namely, the saddle index  $\delta = 0$ , the decreasing rate of the amplitude of the oscillation curve is smaller than that as  $0 < \delta < 1$ , which means there are more periodic orbits near the homoclinic orbit as  $|\mu| \ll 1$ , and  $\delta = 0$ .

In the following, we consider the existence of the double-pulse homoclinic orbits. According to the global map  $T_1$ , when the homoclinic orbit is broken under certain perturbation, the unstable manifold intersects  $\Sigma_0$  at the point  $M^+(\bar{x}, 0, \mu)$ , thus if  $\mu > 0$ , this point can be used as an initial condition for the next map. The next point of intersection (i.e. the point  $TM^+(\mu)$ ) has the coordinate

$$\begin{aligned} x &= \bar{x} + F(\bar{x}, \mu, 0)A_1 \cos(\Omega \ln \mu + \theta), \\ z &= \mu + F(\bar{x}, \mu, 0)B_1 \sin(\Omega \ln \mu). \end{aligned} \tag{3.3}$$

The condition of existence of a double-pulse homoclinic orbit is  $TM^+ \in W_{loc}^s$ ; i.e.,  $z = 0$ . That is, the new homoclinic orbit passes once through a neighborhood of the origin before falling back into the origin. This condition is given by

$$-\mu = F(\bar{x}, \mu, 0)B_1 \sin(\Omega \ln \mu). \tag{3.4}$$

By a similar analysis, we get a countable infinity of  $\mu$  values

$$\mu_i, \mu_{i+1}, \dots, \mu_{i+n}, \dots \rightarrow 0,$$

for which these double homoclinic orbits exist.

Actually, in order to isolate the solutions of (3.4), we assume

$$\Omega \ln \mu = -2\pi j + \xi,$$

or

$$\mu = e^{-\frac{2\pi j}{\Omega}} e^{\frac{\xi}{\Omega}},$$

where  $j$  is an integer (large enough since  $\mu$  should be small), and  $\xi \in [-\frac{\pi}{2}, \frac{3\pi}{2}]$ . Then equation (3.4) is rewritten as

$$\sin \xi = -\frac{1}{B_1} F^{-1}(\bar{x}, \mu, 0) e^{-\frac{2\pi j}{\Omega}} e^{\frac{\xi}{\Omega}}. \tag{3.5}$$



Note that the quantity  $F^{-1}(\bar{x}, \mu, 0)e^{-\frac{2\pi j}{\Omega}}$  is very small when  $j$  is large enough. Hence, equation (3.5) has exactly two solutions  $\xi_1, \pi - \xi_1$  on the interval  $-\frac{\pi}{2} \leq \xi \leq \frac{3\pi}{2}$ , where

$$\xi_1 = -\frac{1}{B_1}F^{-1}(\bar{x}, \mu, 0)e^{-\frac{2\pi j}{\Omega}} + \dots .$$

Substituting these expressions into equation  $\mu = e^{-\frac{2\pi j}{\Omega}}e^{\frac{\xi}{\Omega}}$ , we find an infinite series of bifurcation curves  $\{L_j^0(\mu), L_j^1(\mu)\}$  which correspond to the existence of double-pulse homoclinic orbits.

Finally, we consider homoclinic connections to periodic orbit as  $\lambda > 0$ .

From hypothesis (H<sub>1</sub>), by a supercritical Hopf bifurcation, the periodic orbit, which exists for  $\lambda > 0$ , is denoted approximately by  $C = \{r = \sqrt[2k]{\lambda}, z = 0\}$  with local coordinates  $r, z$ . Note that close to the equilibrium or close to the periodic orbit, the invariant manifolds have very simple expressions using the coordinates given in hypothesis (H<sub>1</sub>). Now the equation  $z = 0$  corresponds the two dimensional stable manifolds of  $C$  and the cylinder  $x^2 + y^2 = \lambda^{\frac{1}{k}}$  is the unstable manifold of  $C$  (see [8]). The periodic orbit  $C$  is a hyperbolic orbit whose trajectory is given by  $x^2 + y^2 = \lambda^{\frac{1}{k}}$ , and  $z = 0$ . A trivial parameterization of this curve is

$$(x(s), y(s), z(s)) = (\sqrt[2k]{\lambda} \cos(s), \sqrt[2k]{\lambda} \sin(s), 0) \quad \text{for } s \in [0, 2\pi).$$

The unstable manifold of  $C$  intersects  $\Sigma_1$  with coordinates  $(\sqrt[2k]{\lambda} \cos(s), \sqrt[2k]{\lambda} \sin(s), \varepsilon)$ . A homoclinic connection will exist if one of the points of the circle is mapped by  $T$  onto  $z = 0$ , i.e.,

$$c \sqrt[2k]{\lambda} \cos(s) + d \sqrt[2k]{\lambda} \sin(s) + \mu = 0,$$

then we have

$$\sqrt[2k]{\lambda} B_1 \sin(s + \phi) = \mu,$$

where  $B_1 = \sqrt{c^2 + d^2}$ ,  $\cos \phi = -\frac{d}{B_1}$ ,  $\sin \phi = -\frac{c}{B_1}$ .

If a value of  $s$  is fixed in this equation, then a parameter curve  $\mu = \mu(\lambda)$  of the existence of homoclinic connection to  $C$  is obtained.

**Acknowledgements** The authors would like to thank the referees for their helpful comments and suggestions.

## References

- [1] Algaba, A., Merino, M., Rodriguez-Luis, A. J.: Homoclinic connections near a Belykov point in Chua's equation. *Int. J. Bifur. Chaos*, **15**, 1239–1252 (2005)
- [2] Algaba, A., Merino, M., Rodriguez-Luis, A. J.: Analysis of a Belykov homoclinic connection with  $Z_2$ -symmetry. *Nonlinear Dynam.*, **69**, 519–529 (2012)
- [3] Belykov, L. A.: The bifurcation set in a system with a homoclinic saddle curve. *Math. Z.*, **28**, 910–916 (1980)
- [4] Belykov, L. A.: Bifurcation of system with homoclinic curve of a saddle-focus with saddle quantity zero. *Math. Z.*, **36**, 838–843 (1984)
- [5] Champney, A. R., Rodriguez-Luis, A. J.: The non-transverse Sil'nikov–Hopf bifurcation: uncoupling of homoclinic orbits and homoclinic tangencies. *Phys. D*, **128**, 130–158 (1999)
- [6] Chen, F. J., Zhou, L. Q.: Strange attractors in a periodically perturbed Lorenz-Like equation. *J. Appl. Analysis Comput.*, **2**, 123–132 (2013)
- [7] Deng, B., Sakamoto, K.: Sil'nikov–Hopf bifurcations. *J. Differential Equations*, **119**, 1–23 (1995)

- [8] Fernández-Sánchez, F., Freire, E., Rodríguez-Luis, A. J.: Analysis of the T-point-Hopf bifurcation. *Phys. D*, **237**, 292–305 (2008)
- [9] Glendinning, P., Sparrow, C.: Local and global behavior near homoclinic orbits. *J. Stat. Phys.*, **35**, 645–696 (1984)
- [10] Han, M. A., Zhu, H. P.: The loop quantities and bifurcations of homoclinic loops. *J. Differential Equations*, **234**, 339–359 (2007)
- [11] Hirschberg, P., Knobloch, E.: Sil’nikov–Hopf bifurcations. *Phys. D*, **62**, 202–216 (1993)
- [12] Homburg, A. J., Sandstede, B.: Homoclinic and Heteroclinic Bifurcations in Vector Fields; in: Broer, Henk (ed.) et al., *Handbook of Dynamical Systems*. **3**, Amsterdam: Elsevier, 379–524 (2010)
- [13] Knobloch, J., Lloyd David, J. B., Sandstede, B., et al.: Isolas of 2-pulse solutions in homoclinic snaking scenarios. *J. Dynam. Differential Equations*, **23**, 93–114 (2011)
- [14] Li, J. B., Jiang, L.: Exact solutions and bifurcations of a modulated equation in a discrete nonlinear electrical transmission line (I). *Int. J. Bifur. Chaos.*, **25**, 1550016, 11 pp (2015)
- [15] Liu, X. B., Shi, L. N., Zhang, D. M.: Homoclinic flip bifurcation with a nonhyperbolic equilibrium. *Nonlinear Dynam.*, **69**, 655–665 (2012)
- [16] Shen, J., Lu, K. N.; Zhang, W. N.: Heteroclinic chaotic behavior driven by a Brownian motion. *J. Differential Equations*, **255**, 4185–4225 (2013)
- [17] Shilnikov, L. P.: A case of the existence of a countable number of periodic motions. *Sov. Math. Dokl.*, **6**, 163–166 (1965)
- [18] Shilnikov, L. P.: A contribution to the problem of the structure of an extended neighborhood of a rough equilibrium state of saddle-focus type. *Math. Ussr. Sbornik.*, **10**, 91–102 (1970)
- [19] Stephen, S., Sourdis, C.: Heteroclinic orbits in slow-fast Hamiltonian systems with slow manifold bifurcations. *J. Dynam. Differential Equations.*, **22**, 629–655 (2010)
- [20] Wiggins, S.: *Introduction to Applied Nonlinear Dynamical Systems and Chaos*, Springer-Verlag, New York, 1990
- [21] Xu, Y. C., Zhu, D. M., Liu, X. B.: Bifurcations of multiple homoclinics in general dynamical systems. *Discrete Contin. Dyn. Syst.*, **30**(3), 945–963 (2011)
- [22] Yang, J. M., Xiong, Y. Q., Han, M. A.: Limit cycle bifurcations near a 2-polycycle or double 2-polycycle of planar systems. *Nonlinear Anal.*, **95**, 756–773 (2014)
- [23] Yang, Q. G., Chen, Y. M.: Complex dynamics in the unified Lorenz-type system. *Int. J. Bifur. Chaos.*, **24**, 1450055, 30 pp (2014)
- [24] Zhu, D. M., Wang, F. J.: Global bifurcation in the shil’nikov phenomenon with weak attractivity. *Appl. Math. J. Chinese Univ. Ser. A*, **3**, 256–265 (1994)